Int. J. Electrochem. Sci., 6 **(2011)** 931 - 957

International Journal of
ELECTROCHEMICAL
SCIENCE
www.electrochemsci.org

QSAR, Experimental and Computational Chemistry Simulation Studies on the Inhibition Potentials of Some Amino Acids for the Corrosion of Mild Steel in 0.1 M HCl

Nnabuk O. Eddy [1,*], *Femi E. Awe*[1], *Casmir. E. Gimba*[1], *Nkechi O. Ibisi*[2], *Eno E. Ebenso*[3,*]

[1] Department of Chemistry, Ahmadu Bello University, Zaria, Nigeria
[2] Department of Chemistry, Michael Okpara University of Agriculture,Umudike, Nigeria
[3] Department of Chemistry, North West University (Mafikeng Campus), Private Bag X2046, Mmabatho 2735, South Africa
[*]E-mails: nabukeddy@yahoo.com, Eno.Ebenso@nwu.ac.za

Received: 13 February 2011 / *Accepted:* 2 March 2011 / *Published:* 1 April 2011

Inhibition and adsorption potentials of cysteine, glycine, leucine and alanine for the corrosion of mild steel in hydrochloric acid (HCl) solution were investigated using experimental and quantum chemical approaches. The experimental study was carried out using gravimetric, gasometric, thermometric and Fourier transformed infra red (FTIR) methods while the quantum chemical study was carried out using semi-empirical, ab-initio and quantitative structure activity relation (QSAR) methods. The results obtained indicated that various concentrations of the studied amino acids inhibited the corrosion of mild steel in HCl solution through physiosorption. The inhibition potentials of the inhibitors decreased in the order, cysteine > leucine > alanine > glycine. The adsorption of the inhibitors on mild steel surface was found to be exothermic, spontaneous and supported the Langmuir adsorption model. Results obtained from quantum chemical studies showed excellent correlations between quantum chemical parameters and experimental inhibition efficiencies (for gas and aqueous phases using density functional theory (DFT) and Moller-Plesset (MP2) perturbations). Correlations between the experimental inhibition efficiencies and theoretical inhibition efficiencies (obtained from QSAR) were also excellent.

Keywords: Corrosion, inhibition, amino acids, computational chemistry simulation

1. INTRODUCTION

Corrosion inhibitors are needed in the oil, fertilizer, metallurgical and other industries [1]. This is because during some industrial processes, valuable metals (such as aluminium, mild steel and zinc)

are made to come in contact with aggressive media (such as acids, bases or salts), and are therefore prone to corrosion attack [3,4].

In order to prevent the environmental damages caused by corrosion, several steps have been adopted. However, the use of inhibitors has been found to be one of the best options of protecting metals against corrosion [5]. Most corrosion inhibitors are organic compounds which slow down the rate of corrosion of a metal through the mechanism of adsorption [6]. Also, they have hetero atoms (such as N, O, S and P) in their aromatic or long carbon chain systems. The presence of hetero atoms and suitable functional groups can facilitate the adsorption of the inhibitor on the metal surface [7].

Over the years, numerous classes of inhibitors have been investigated. However, the trend in green chemistry is concentrated towards the replacement of most of these inhibitors with the non toxic, cheap and eco-friendly inhibitors. In the light of this, some plant extract have been found to meet these requirements [8, 9]. Recent studies have also given hopes on the use of amino acids as inhibitors for the corrosion of metals [10-18]. However, in spite of the huge success that has been attributed to the use of computational chemistry in corrosion studies, most of the ongoing researches on the inhibitory potentials of amino acids are restricted to laboratory work. Therefore, the present study is aimed at investigating the inhibitory and adsorption properties of L-leucine (LEU), glycine (GLY), L-cysteine (CYS) and L-alanine (ALA) for the corrosion of mild steel using experimental and quantum chemical principles. Gravimetric method shall be used to ascertain the average inhibition potentials of the amino acids while gasometric and thermometric methods shall be used to study the instantaneous inhibition potentials of the amino acids. Studies on the adsorption behaviour of the inhibitors were carried out using FTIR spectroscopy. Theoretical studies involved the correlation between experimental results and semi-empirical parameters; the analysis of the sites for electrophilic and nucleophilic attacks carried out using Fukui function and the derivation of equations for the theoretical inhibition efficiencies of the inhibitors using the quantitative structure activity relation (QSAR).

2. EXPERIMENTAL

2.1. Materials

Materials used for the study were mild steel sheet of composition (wt %); Mn (0.6), P (0.36), C (0.15) and Si (0.03) and the rest Fe. The sheet was polished and mechanically pressed cut into different coupons, each of dimension, $5 \times 4 \times 0.11$cm. Each coupon was degreased by washing with ethanol, dipped in acetone and allowed to dry in the air before they were preserved in a desicator. All reagents used for the study were Analar grades and double distilled water was used for their preparation.

The concentrations of the inhibitors were within the range, 1 to 5 g/l. Each of these concentrations were used to prepare different test solutions by dissolving them in 0.1 M HCl (for use in gravimetric analysis) and in 2.5 M HCl (for use in gasometric and thermometric analyses) respectively.

2.2. Gravimetric method

In the gravimetric experiment, a previously weighed metal (mild steel) coupon was completely immersed in 250 ml of the test solution in an open beaker. The beaker was covered with aluminium foil and was inserted into a water bath maintained at 303 K. After every 24 hours, the corrosion product was removed by washing each coupon (withdrawn from the test solution) in a solution containing 50 % NaOH and 100 g l^{-1} of zinc dust [19]. The washed coupon was rinsed in acetone and dried in the air before re-weighing. The experiment was also repeated at 333 K. In each case, the difference in weight for a period of 168 h was taken as the total weight loss. From the average weight loss results (average of three replicate analysis), the inhibition efficiency (IE_{exp}) of the inhibitor, the corrosion rate of mild steel and the degree of surface coverage were calculated using equations 1, 2 and 3 respectively [20] ;

$$IE_{exp} = (1 - W_1/W_2) \times 100 \quad (1)$$

$$CR = (W_2 - W_1)/At \quad (2)$$

$$\theta = 1 - W_1/W_2 \quad (3)$$

where W_1 and W_2 are the weight losses (g) for mild steel in the presence and absence of the inhibitor respectively, CR is the corrosion rate of mild steel in $gcm^{-2}h^{-1}$, A is the area of the mild steel in cm^2, t is the total period of immersion (in hours) and θ is the degree of surface coverage of the inhibitor.

2.3. Gasometric method

Gasometric methods were carried out at 303 K using a gasometer. In each case, the metal coupon was inserted into the round bottom flask (containing the test solution) of the gasometer. The volumes of hydrogen gas evolved were measured after every minute until a steady value was obtained. From the volume of hydrogen gas evolved per minute, inhibition efficiencies were calculated using equation 4 [21];

$$IE_{exp} = \left(1 - \frac{V_{Ht}^{1}}{V_{Ht}^{o}}\right) x\,100 \quad (4)$$

where V_{Ht}^{1} and V_{Ht}^{o} are the volumes of H_2 gas evolved at time, 't' for inhibited and uninhibited solutions respectively.

2.4. Thermometric method

This was carried out using a thermometric flask. From the rise in temperature of the system per minute, the reaction number (RN) was calculated using equation 5 [22]:

$$RN\left(^{o}C\ \min^{-1}\right) = \frac{T_m - T_i}{t} \qquad 5$$

where T_m and T_i are the maximum and initial temperatures respectively and 't' is the time (min) taken to reach the maximum temperature. The inhibition efficiency (%I) of the inhibitor was evaluated from percentage reduction in the reaction number as follows.

$$\%I = \frac{RN_{aq} - RN_{wi}}{RN_{aq}} \times 100 \qquad 6$$

where RN_{aq} is the reaction number in the absence of inhibitors (blank solution) and RN_{wi} is the reaction number of 2.5 M HCl containing the studied inhibitors.

2.5. Computational techniques

Single point energy calculations were carried out using Austin model 1(AM1), parametric method 6 (PM6), parametric method 3 (PM3), modified neglect of diatomic overlap (MNDO) and recief model 1 (RM1) Hamiltonians in the MOPAC 2008 software for Windows [23]. Calculations were performed on an HP Pentium V (2.0 GHz, 4 GB RAM and 250 GB hard disc) computer. Semi-empirical parameters calculated (for gas and aqueous phases) were, the energy of the highest occupied molecular orbital (E_{HOMO}), the energy of the lowest unoccupied molecular orbital (E_{LUMO}), the dipole moment (μ), the total energy (TE), the electronic energy (EE), the core core repulsion energy (CCR), the ionization potential (IP), the cosmo area (cosAr) and the cosmo volume (CosVol). The Mulliken and Lowdin charges (q) for nucleophillic and electrophillic attacks were computed using GAMESS computational software using COSMO solvation model [24]. Correlation type and method used for the calculation were MP2 and DFT while the basis sets were fixed at 6-13G and STO-5G respectively.

Statistical analyses were performed using SPSS program version 15.0 for Windows. Non-linear regression analyses were performed by unconstrained sum of squared residuals for loss function and estimation methods of Levenberg-Marquardt using SPSS program version 15.0 for Windows.

3. RESULTS AND DISCUSSIONS

3.1. Effect of concentration of amino acids

Fig. 1 shows the variation of weight loss of mild steel with time for the corrosion of mild steel in 0.1 M HCl containing various concentrations of the studied amino acids. From the plots, it is evident that weight loss of mild steel decreases with increase in the concentration of the amino acid but increases with increasing period of contact. These indicate that the rate of corrosion of mild steel in 0.1 M HCl increases with increase in the period of contact but decreases with increase in the concentration

of the studied amino acids. Therefore the studied amino acids inhibited the corrosion of mild steel in HCl solutions. Table 1 presents values of the inhibition efficiencies of the studied amino acids.

Table 1. Corrosion rates, inhibition efficiencies and some thermodynamic parameters of the studied amino acids

System	Inhibition efficiency (%)				Corrosion rate ($gh^{-1}cm^{-2}$) x 10^{-4}				E_a (kJ/mol)			
	CYS	GLY	LEU	ALA	CYS	GLY	LEU	ALA	CYS	GLY	LEU	ALA
Blank at 303 K	-	-	-	-	4.48	4.48	4.48	4.48	49.66			
0.1g/l at 303K	78.42	50.06	54.22	52.30	1.17	2.24	2.19	2.14	53.94	55.85	55.10	54.72
0.2 g/l at 303 K	73.93	50.56	55.83	53.58	0.97	2.20	1.74	2.08	53.54	57.64	57.29	55.85
0.3 g/l at 303 K	79.00	54.75	59.50	53.75	0.94	2.21	1.72	2.07	55.85	58.66	57.64	57.29
0.4 g/l at 303 K	82.09	55.91	60.59	54.02	0.802	1.97	1.63	2.06	57.64	59.64	60.90	58.32
0.5 g/l at 303 K	82.21	56.50	64.42	56.56	0.79	1.95	1.61	194	58.99	60.90	61.51	60.59
Blank at 333 K	-	-	-	-	26.86	26.86	26.86	26.86				
0.1g/l at 333K	69.59	41.75	43.05	44.36	8.17	15.65	15.30	14.95				
0.2 g/l at 333 K	74.82	42.33	57.47	45.85	6.76	15.49	12.19	14.54				
0.3 g/l at 333 K	75.51	42.56	54.55	46.06	6.58	15.43	12.21	14.49				
0.4 g/l at 333 K	79.10	48.57	54.62	46.37	5.61	13.81	11.42	14.41				
0.5 g/l at 333 K	79.25	49.26	57.95	49.33	5.57	13.63	11.30	13.61				
System	Gasometric (IE_{exp})				Thermometric (IE_{exp})				Q_{ads} (kJ/mol)			
	CYS	GLY	LEU	ALA	CYS	GLY	LEU	ALA	CYS	GLY	LEU	ALA
0.1g/l at 303K	82.34	60.23	60.02	61.23	80.21	59.34	61.02	59.08	-4.50	-23.84	-26.44	-19.40
0.2 g/l at 303 K	84.44	63.21	63.45	64.22	83.45	62.34	63.24	63.43	-5.38	-17.33	-11.21	-14.37
0.3 g/l at 303 K	87.03	64.34	63.55	66.90	86.32	64.33	66.22	66.39	-4.64	-14.09	-8.77	-9.88
0.4 g/l at 303 K	90.00	64.44	64.43	67.00	88.94	68.39	69.01	69.87	-8.69	-14.47	-5.61	-11.85
0.5 g/l at 303 K	93.42	66.22	70.21	69.21	92.01	72.98	70.54	73.21	-7.80	-8.66	-16.14	-7.96

From Table 1, it can be seen that inhibition efficiencies of the studied amino acids increase with concentration but decrease with increasing temperature. These indicate that the studied amino acids are adsorption inhibitors and that their adsorption on mild steel surface supports the mechanism of physical adsorption [25]. Table 1 also reveals that the order for the increase in inhibition efficiency of the studied amino acids is CYS >LEU >ALA > GLY.

Gravimetric results (weight loss) discussed above, are concerned with the average inhibition efficiency of the amino acids. Gasometric and thermometric methods measure instantaneous inhibition efficiency (i.e inhibition efficiency over a short period). In Table 1, values of the instantaneous inhibition efficiencies (obtained from gasometric and thermometric measurements) of CYS, GLY, LEU and ALA are presented. The results obtained are comparable to those obtained from gravimetric measurements. However, the inhibition efficiencies obtained from the latter are relatively higher than those obtained from gravimetric measurements indicating that the instantaneous inhibition efficiencies of the studied amino acids are better than their average inhibition efficiencies.

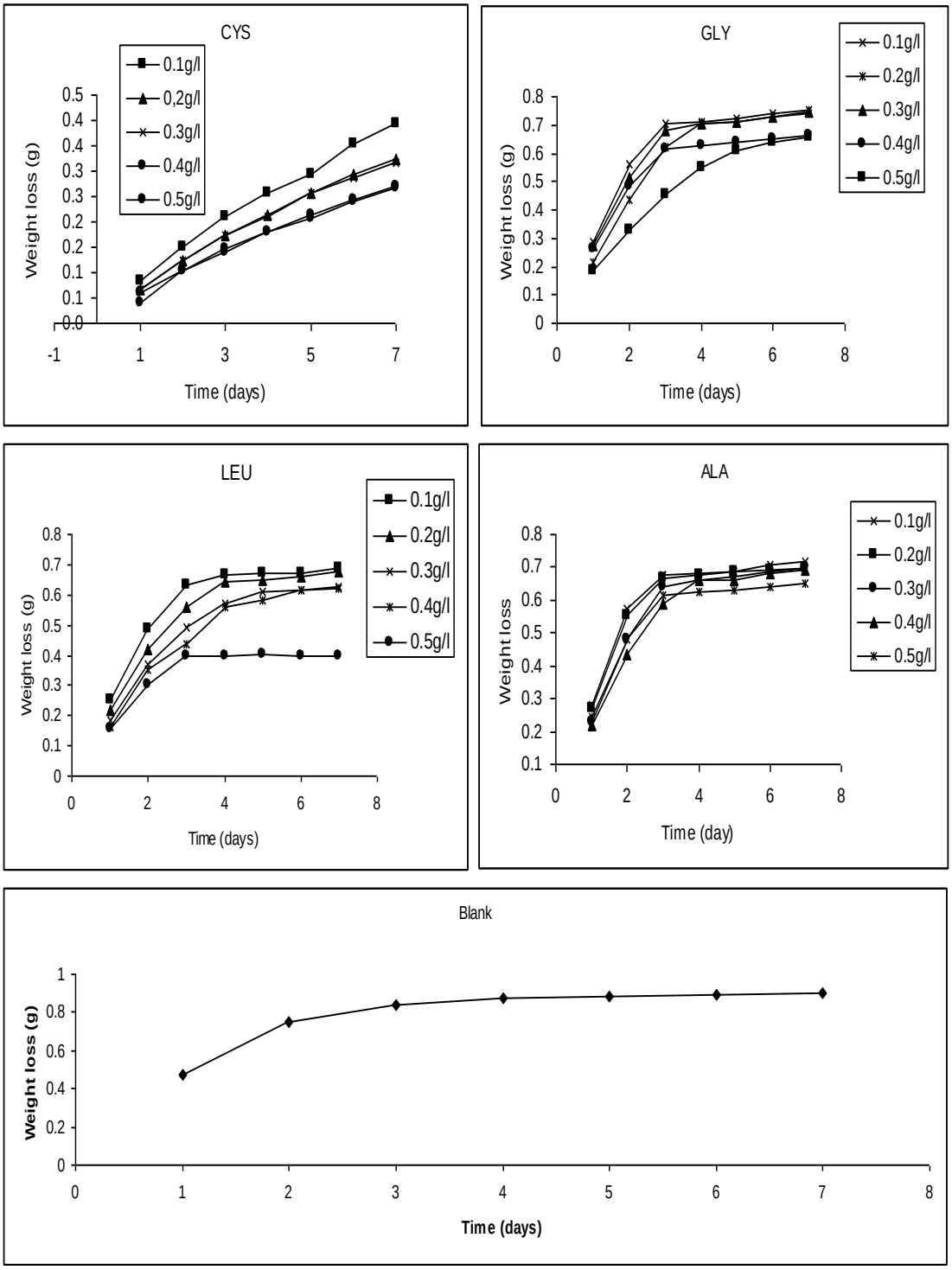

Figure 1. Variation of weight loss of mild steel with time for the corrosion of mild steel in 0.1 M HCl containing various concentrations of amino acids at 303 K

3.2. Effect of temperature

The effect of temperature on the corrosion of mild steel in 0.1 M HCl was investigated using the logarithm form of the Arrhenius equation, which can be written as follows [26];

$$\log(CR_2/CR_1) = E_a/2.303R\ (1/T_1 - 1/T_2) \quad 7$$

where CR_1 and CR_2 are the corrosion rates of mild steel at the temperatures, T_1(303 K) and T_2 (333 K), R is the molar gas constant and E_a is the activation energy. The activation energies calculated from equation 7 are recorded in Table 1. The activation energies are less than the threshold value (80 $kJmol^{-1}$) required for the mechanism of chemical adsorption. Therefore, the adsorption of the studied amino acids on mild steel surface is consistent with the mechanism of charge transfer from the charged inhibitor's molecule to the charged metal surface, which represents physiosorption.

3.3. Thermodynamics/adsorption study

The heat of adsorption of the inhibitors was calculated using the following equation [27],

$$Q_{ads} = 2.303R\left[\log\left(\frac{\theta_2}{1-\theta_2}\right) - \log\left(\frac{\theta_1}{1-\theta_1}\right)\right] x\left(\frac{T_{1X}T_2}{T_2 - T_1}\right) kJmol^{-1} \quad 8$$

where R is the molar gas constant, θ_1 and θ_2 are the degrees of surface coverage of the inhibitor at the temperatures T_1 (303 K) and T_2 (333 K). Calculated values of Q_{ads} recorded in Table 1, are negative indicating that the adsorption of the studied amino acids on mild steel surface is exothermic.

The adsorption characteristics of the studied amino acids were investigated by fitting data obtained for the degree of surface coverage into different adsorption isotherms. The tests revealed that the adsorption of the amino acids on mild steel surface is best described by Langmuir adsorption isotherm. Langmuir adsorption model can be represented as follows [28];

$$\log(C/\theta) = \log C - \log k_{ads} \quad 9$$

Using equation 9, plots of log(C/θ) versus logC were linear (plots not shown). Values of adsorption parameters deduced from the plots are presented in Table 2. The results obtained, revealed that the slopes and R^2 values for the isotherms are very close to unity, confirming the application of the Langmuir model to the adsorption of the studied amino acids.

The equilibrium constant of adsorption (obtained from the intercept of the Langmuir adsorption isotherm) is related to the free energy of adsorption according to the following equation [29],

$$\Delta G^0_{ads} = -2.303RT\log(55.5K_{ads}) \quad 10$$

Calculated values of ΔG^0_{ads} are also presented in Table 2. From the results obtained, the free energies are negatively less than the threshold value of -40 $kJmol^{-1}$ required for the mechanism of chemical adsorption. Therefore, the adsorption of the amino acids on mild steel surface is spontaneous and favours the mechanism of physical adsorption [30].

Table 2. Langmuir parameters for the adsorption of the studied amino acids on mild steel surface at 303 and 333 K

T (K)		Slope	$\log k_{ads}$	R^2	ΔG^0_{ads} (kJmol^{-1})
303 K	CYS	0.9585	0.0778	0.9968	-1.51
	GLY	0.90707	0.2612	0.9917	-1.75
	LEU	0.8523	0.1389	0.9793	-1.59
	ALA	0.9614	0.2448	0.9994	-1.73
333 K	CYS	0.9183	0.00739	0.9997	-1.55
	GLY	0.8937	0.2868	0.9938	-1.96
	LEU	0.8213	0.1695	0.9929	-1.79
	ALA	0.9475	0.3031	0.9999	-1.98

3.4. FTIR study

FTIR analysis was carried out using the corrosion product (in the absence and presence of the inhibitor) and the inhibitor. The FTIR spectrum of the corrosion product of mild steel (Figure not shown) did not show any adsorption peak indicating that the corrosion product of mild steel is not infra red active. However, Fig. 2 (a) shows the IR spectrum of CYS while Fig. 2 (b) shows the IR spectrum of the corrosion product of mild steel when 0.5 g/l of CYS was used as an inhibitor. From the frequencies and peaks of IR adsorption deduced from the spectra, it is evident that in CYS, the N-H wag at 779.27, 846.78 and 873.78 cm^{-1} were shifted to 868.00 cm^{-1}, C-N stretch at 1194.94 cm^{-1} was shifted to 2372.52 cm^{-1}, the O-H stretch at 2579.88 and 3136.36 cm^{-1} were shifted to 2970.48 cm^{-1} while the O-H stretch at 3448.84 cm^{-1} was shifted to 3425.69 cm^{-1} indicating that there is an interaction between CYS and mild steel surface. On the other hand, the N-O asymmetric stretch at 1475.59 cm^{-1}, the C-N stretch at 1041.60, 1126.47 and 1194.94 cm^{-1} were missing in the spectrum of the corrosion product indicating that these bonds might have been used for adsorption [31].

Figs. 3 (a) and 3 (b) respectively show the FTIR spectra of GLY and that of the corrosion product of mild steel when GLY was used as an inhibitor. From the peaks and frequencies of IR adsorption deduced from the spectra, it was found that the C-O stretch at 1042.56 cm^{-1} was shifted to 1028.09 cm^{-1}, the –C=C- stretch at 1674.27 cm^{-1} was shifted to 1656.91 cm^{-1}, the O-H stretch at 2906.82 cm^{-1} was shifted to 2924.18 cm^{-1} while the O-H stretch (H-bonded) was shifted from 3201.94 to 3430.51 cm^{-1}. These shifts in frequencies also indicate that there is an interaction between GLY and the metal surface. It was also found that the C-N stretch (at 1125.50 and 1247.99 cm^{-1}), the C-O stretch (at 1042.56 and 1730.21 cm^{-1}), the N-O symmetric stretch (at 1338.64 cm^{-1}) and the N-H bend at 1590.36 cm^{-1} were missing in the spectrum of the corrosion product indicating that these bonds were used for the adsorption of GLY onto mild steel surface.

Fig. 4 (a) and 4 (b) respectively show the FTIR spectra of LEU and that of the corrosion product of mild steel when LEU was used as an inhibitor. From the results obtained, it can be seen that the N-H wag at 669.32 cm^{-1} was shifted to 675.11 cm^{-1}, C-H bend at 842.92 was shifted to 867.03 cm^{-1}, the C-N stretches at 1084.03 and 1135.50 cm^{-1} were shifted to 1032.92 and 114.89 cm^{-1} respectively,

the O-H stretch at 2888.50 cm^{-1} was shifted to 2927.08 cm^{-1} while the N-H stretch at 3125.75 cm^{-1} was shifted to 3437.26 cm^{-1}.

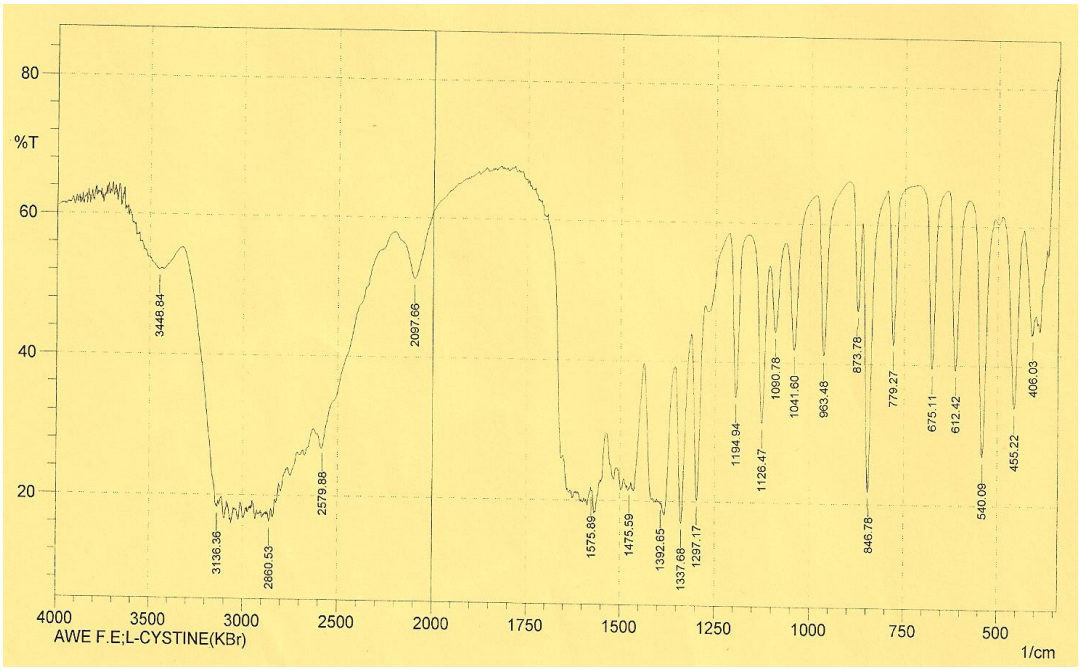

(a)

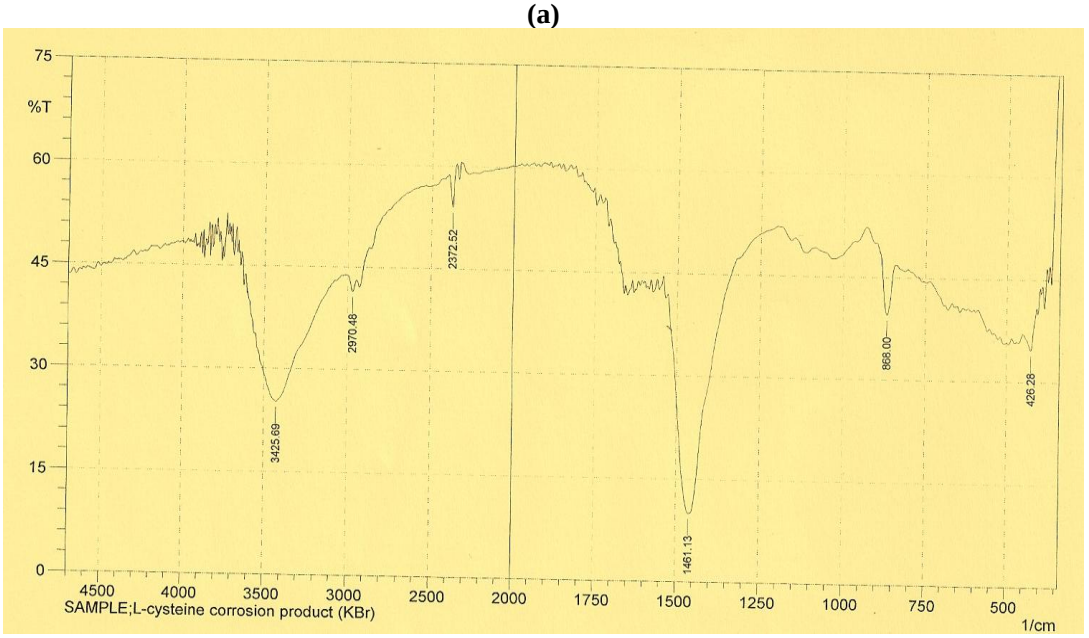

(b)

Figure 2. (a) IR spectrum of CYS (b) IR spectrum of the corrosion product of mild steel when 0.5 g/l of CYS was used as an inhibitor

These shifts in frequencies also indicate that there is an interaction between LEU and mild steel. On the other hand, the absence of C-N stretch, N-O asymmetric and symmetric stretches in the spectrum of the corrosion product suggest that these bonds were involved in the adsorption of LEU onto mild steel surface.

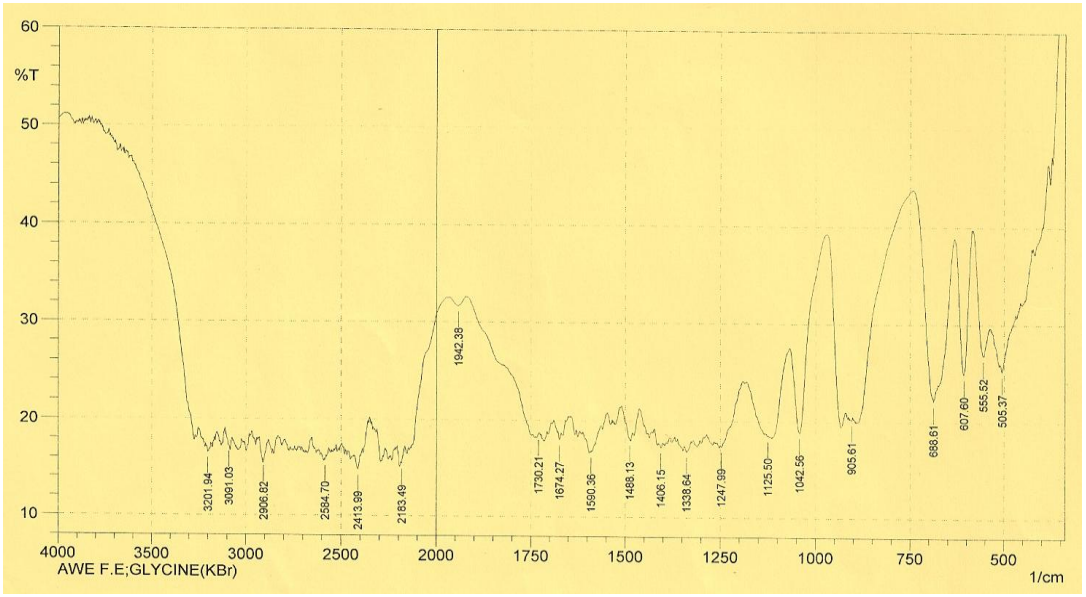

(a)

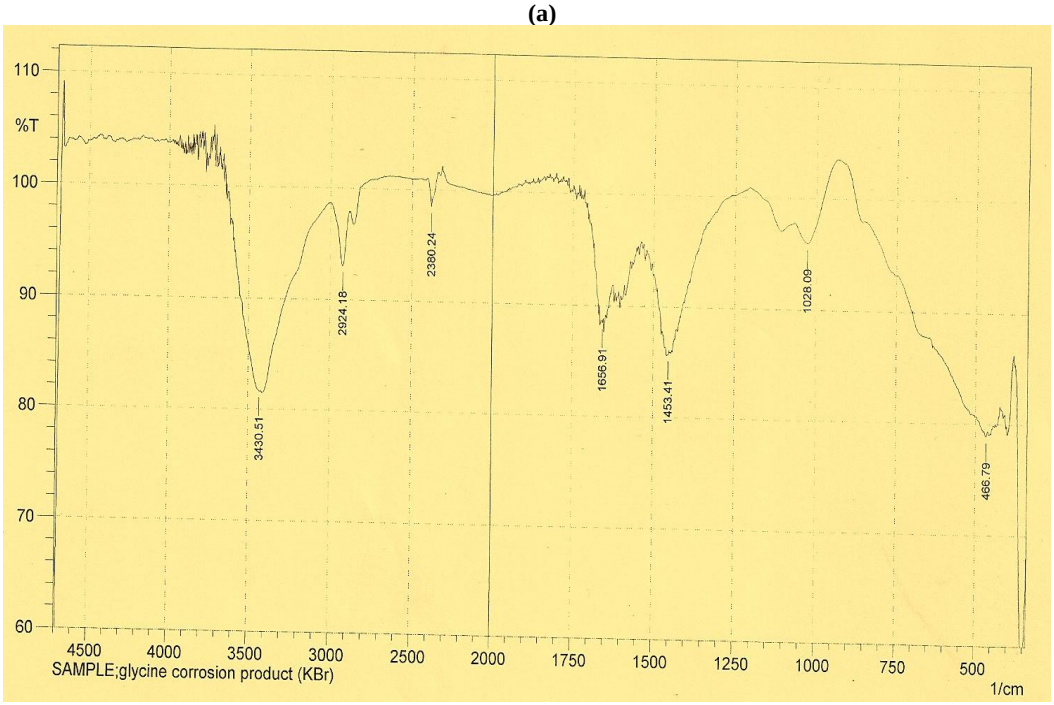

(b)

Figure 3. (a) IR spectrum of GLY, (b) IR spectrum of the corrosion product of mild steel when 0.5 g/l of GLY was used as an inhibitor

The FTIR spectra of ALA and that of the corrosion product of mild steel when ALA was used as an inhibitor are presented in Figs. 5 (a) and 5 (b). From the results obtained, it can be seen that the =C-H bend at 649.07 was shifted to 673.18 cm^{-1}, the C-O stretch at 1017.48 cm^{-1} was shifted to 1030.02 cm^{-1}, the N-H bend at 1614.47 cm^{-1} was shifted to 1652.09 cm^{-1}, the O-H stretch at 2834.49 and 3200.98 cm^{-1} were shifted to 2925.15 and 3428.58 cm^{-1} respectively. In addition, new C-H bend at

1448.59 cm^{-1} were found in the spectrum of the corrosion product. These shifts in frequencies and the formation of a new bond may be due to the interaction between mild steel surface and ALA.

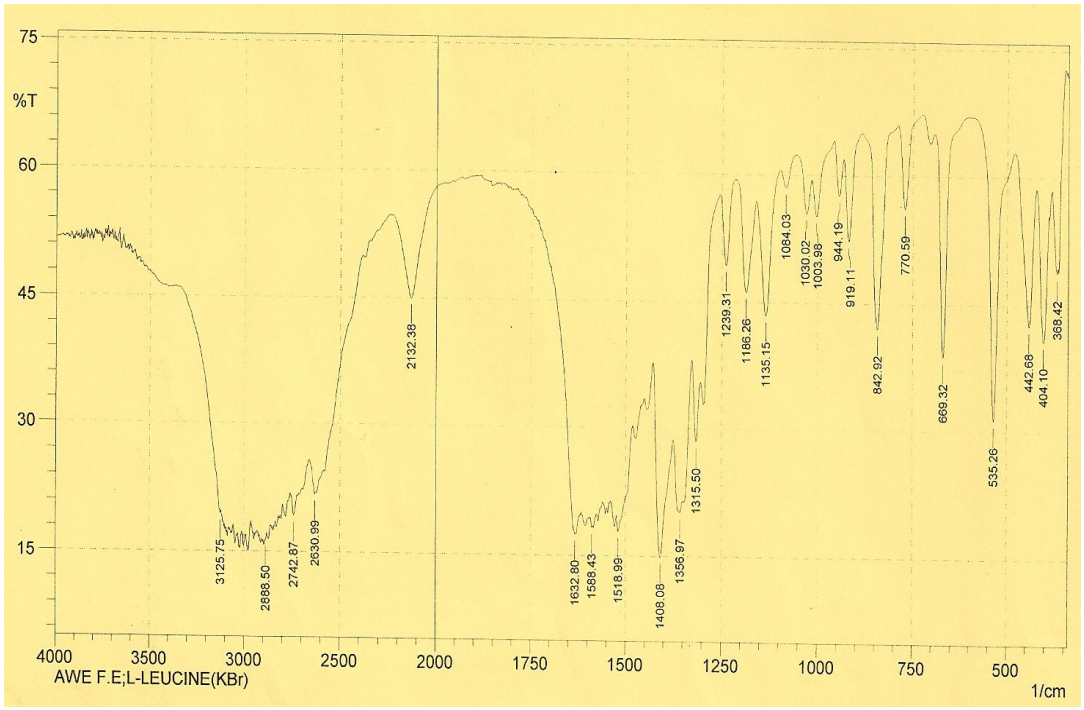

(a)

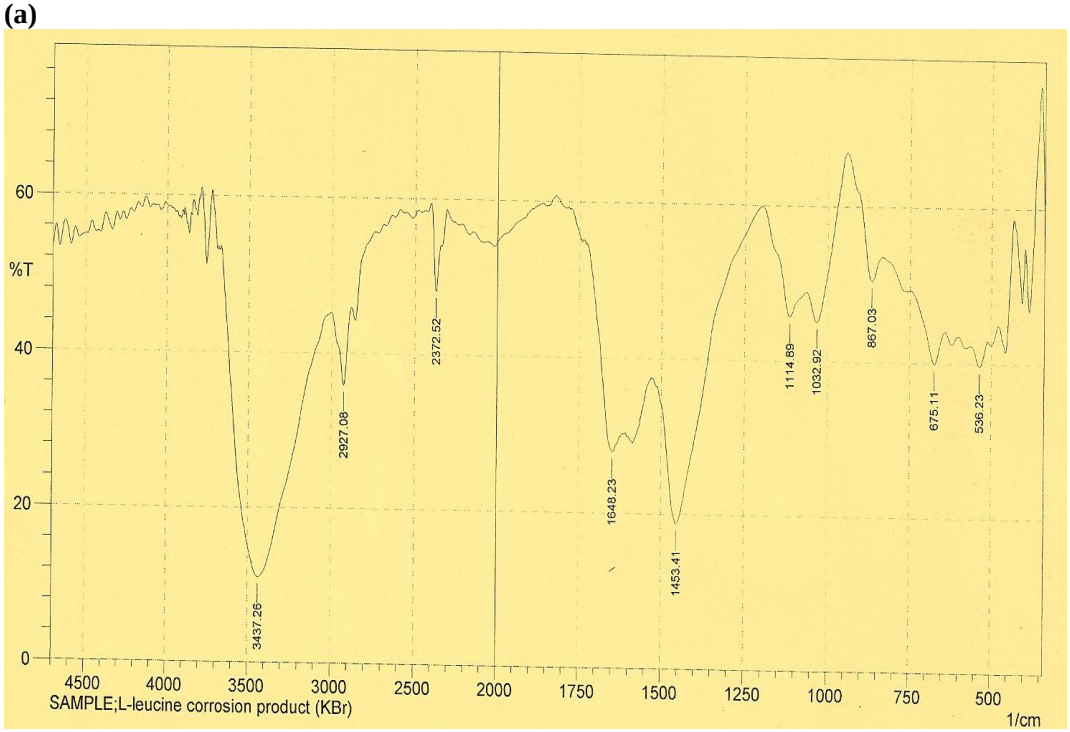

(b)

Figure 4. (a) IR spectrum of LEU, (b) IR spectrum of the corrosion product of mild steel when 0.5 g/l of LEU was used as an inhibitor

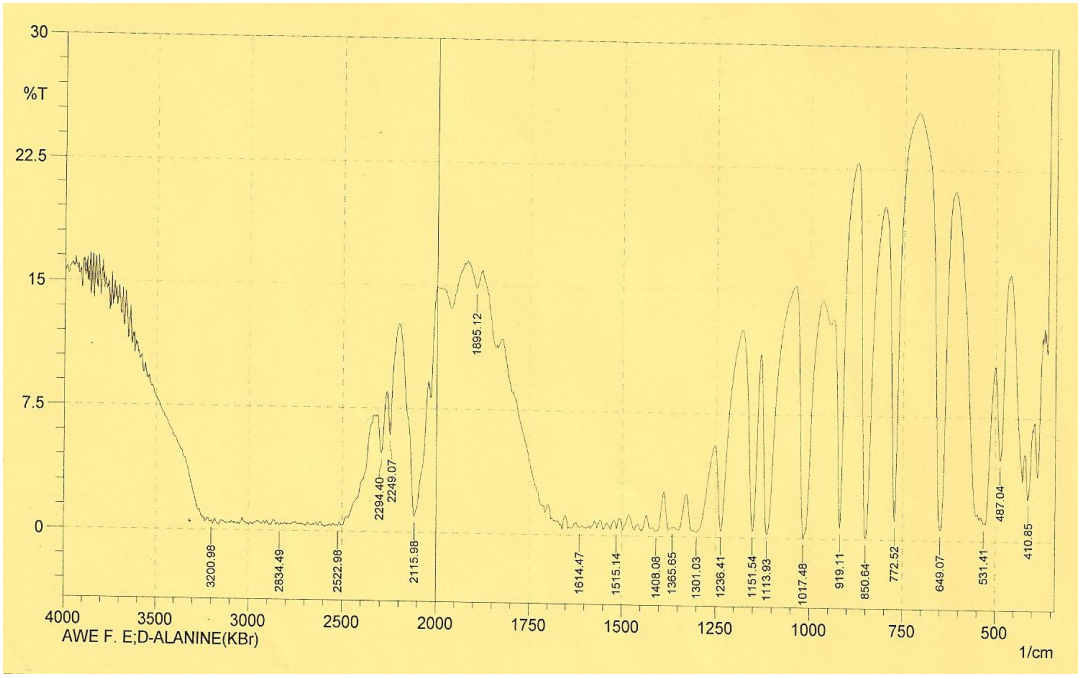

(a)

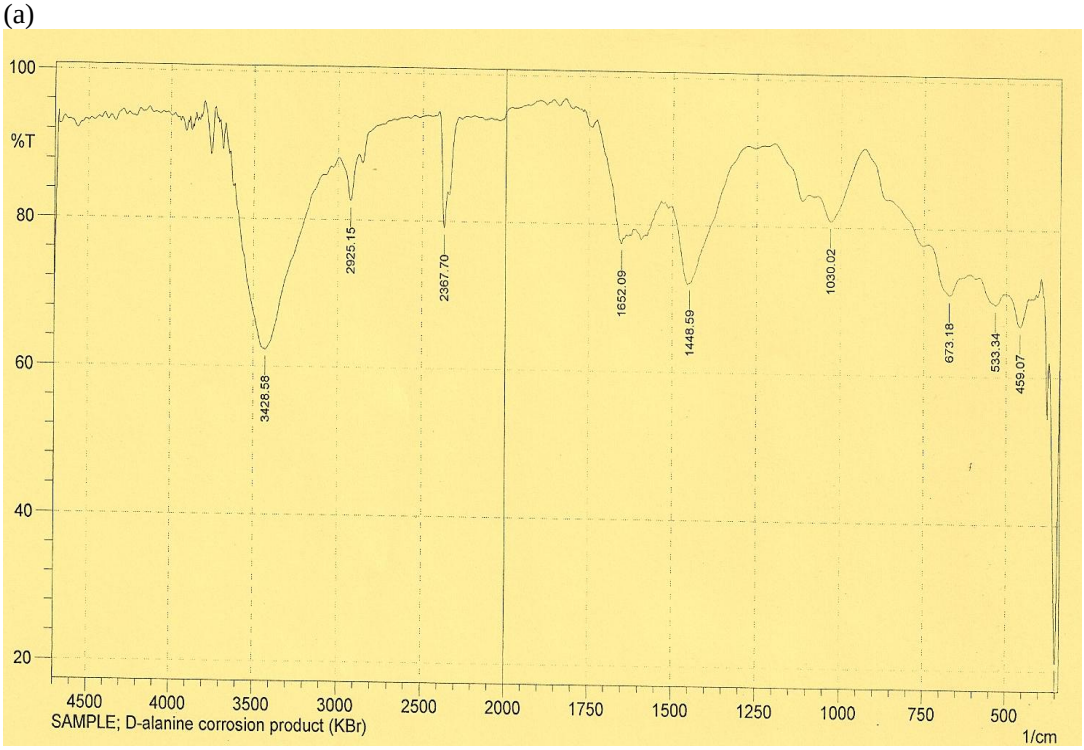

(b)

Figure 5. (a) IR spectrum of ALA, (b) IR spectrum of the corrosion product of mild steel when 0.5 g/l of ALA was used as an inhibitor

On the other hand, the disappearance of C-N stretches at 1113.93 and 1236.41 cm^{-1}, N-O symmetric and asymmetric stretches (at 1301.03 and 1515.14 cm^{-1} respectively), C-H rock at 1365.65 cm^{-1} and O-H stretch at 2522.98 cm^{-1} suggest that some of these bonds might have been used for the adsorption of ALA onto mild steel surface.

3.5. Quantum chemical study

3.5.1. Semi-empirical study

Several quantum chemical parameters such as the electronic energy (EE), core core repulsion energy (CCR), heat of formation (H_f), cosmo area (cosAr) and cosmo volume (cosVol) have been found to be useful in predicting the direction of corrosion reaction. It has been established that corrosion inhibition potentials of structurally related compounds tend to increase or decrease with increase in the value of respective quantum chemical parameter. Table 3 presents values for the frontier molecular orbital energies (i,e E_{HOMO} and E_{LUMO}), ΔE (i.e $E_{LUMO} - E_{HOMO}$), cosAr and μ. The values were obtained for both gas and aqueous phases using PM6, PM3, AM1, RM1 and MNDO Hamiltonians.

Table 3. Quantum chemical parameters for the studied amino in gas and aqueous phases

		Gas phase					Aqueous phase					
	Models	E_{HOMO} (eV)	E_{LUMO} (eV)	ΔE (eV)	CosAr (Å^2)	μ (Debye)	E_{HOMO} (eV)	E_{LUMO} (eV)	ΔE (eV)	CosAr (Å^2)	μ (Debye)	E_{dielec} (eV)
CYS	PM6	-9.04	-0.10	8.94	145.39	2.94	-9.30	-0.20	9.10	145.39	3.82	-0.76
	PM3	-8.98	-0.38	8.60	145.39	3.04	-8.88	-0.33	8.56	145.39	3.83	-0.52
	AMI	-9.00	-0.02	8.98	145.39	2.92	-9.28	0.05	9.33	145.39	3.72	-0.54
	RMI	-9.32	0.17	9.50	145.39	2.80	-9.44	0.21	9.65	145.39	3.64	-0.52
	MNDO	-9.73	0.82	10.56	145.39	2.72	-9.80	0.81	10.61	145.39	3.44	-0.47
GLY	PM6	-8.92	0.46	9.38	104.80	1.92	-9.05	0.24	9.29	104.50	2.78	-0.50
	PM3	-8.64	1.05	9.69	104.80	1.54	-8.63	0.96	9.59	104.50	2.16	-0.32
	AMI	-9.32	1.23	10.55	104.80	1.44	-9.34	1.11	10.45	104.50	1.98	-0.36
	RMI	-9.23	1.17	10.4	104.80	1.41	-9.25	1.06	10.31	104.50	1.96	-0.37
	MNDO	-9.74	1.03	10.77	104.80	1.28	-9.73	0.97	10.7	104.50	1.80	-0.33
LEU	PM6	-8.88	0.53	9.41	131.17	2.23	-9.05	0.22	9.27	172.96	3.00	-0.49
	PM3	-8.64	1.09	9.73	131.17	1.69	-8.70	0.94	9.64	172.96	2.26	-0.31
	AMI	-9.24	1.30	10.54	131.17	1.62	-9.31	1.11	10.42	172.96	2.12	-0.35
	RMI	-9.19	1.24	10.43	131.17	1.63	-9.28	1.06	10.34	172.96	2.14	-0.35
	MNDO	-9.65	1.08	10.73	131.17	1.42	-9.71	0.96	10.67	172.96	1.91	-0.32
ALA	PM6	-9.97	0.49	10.46	121.96	2.02	-9.10	0.22	9.32	121.96	2.80	-0.47
	PM3	-8.68	1.07	9.75	121.96	1.61	-8.71	0.94	9.65	121.96	2.20	-0.31
	AMI	-9.31	1.27	10.58	121.96	1.52	-9.34	1.11	10.45	121.96	2.06	-0.35
	RMI	-9.27	1.21	10.48	121.96	1.51	-9.32	1.05	10.37	121.96	2.04	-0.35
	MNDO	-9.67	1.06	10.73	121.96	1.37	-9.70	0.97	10.67	121.96	1.89	-0.32
R^2	PM6	0.8651	0.9469	0.9651	0.2013	0.9967	0.0883	0.881	0.4507	0.7796	0.9977	0.928
	PM3	0.917	0.9392	0.9201	0.2013	0.5209	0.9029	0.9238	0.9251	0.7796	0.9683	0.9185
	AMI	0.9322	0.9347	0.9466	0.2013	0.9612	0.995	0.9130	0.9402	0.7796	0.9745	0.9165
	RMI	0.83819	0.9327	0.9242	0.2013	0.9707	0.4448	0.9073	0.9291	0.7796	0.9827	0.8869
	MNDO	0.8177	0.9608	0.916	0.2013	0.9542	0.887	0.8345	0.9601	0.7796	0.9645	0.9108

**R^2 = degree of linearity between quantum chemical parameters and IE_{exp}

According to the frontier molecular orbital theory, the formation of a transition state is due to an interaction between the frontier orbitals (HOMO and LUMO) of reacting species [32]. Therefore, the frontier molecular orbitals play significant roles in defining the reactivity of organic compounds. The E_{HOMO} is related to the electron donating ability of the compound. Higher value of E_{HOMO} indicates that the molecule has a higher tendency towards the donation of electron to appropriate acceptor molecules with low energy and empty molecular orbital.

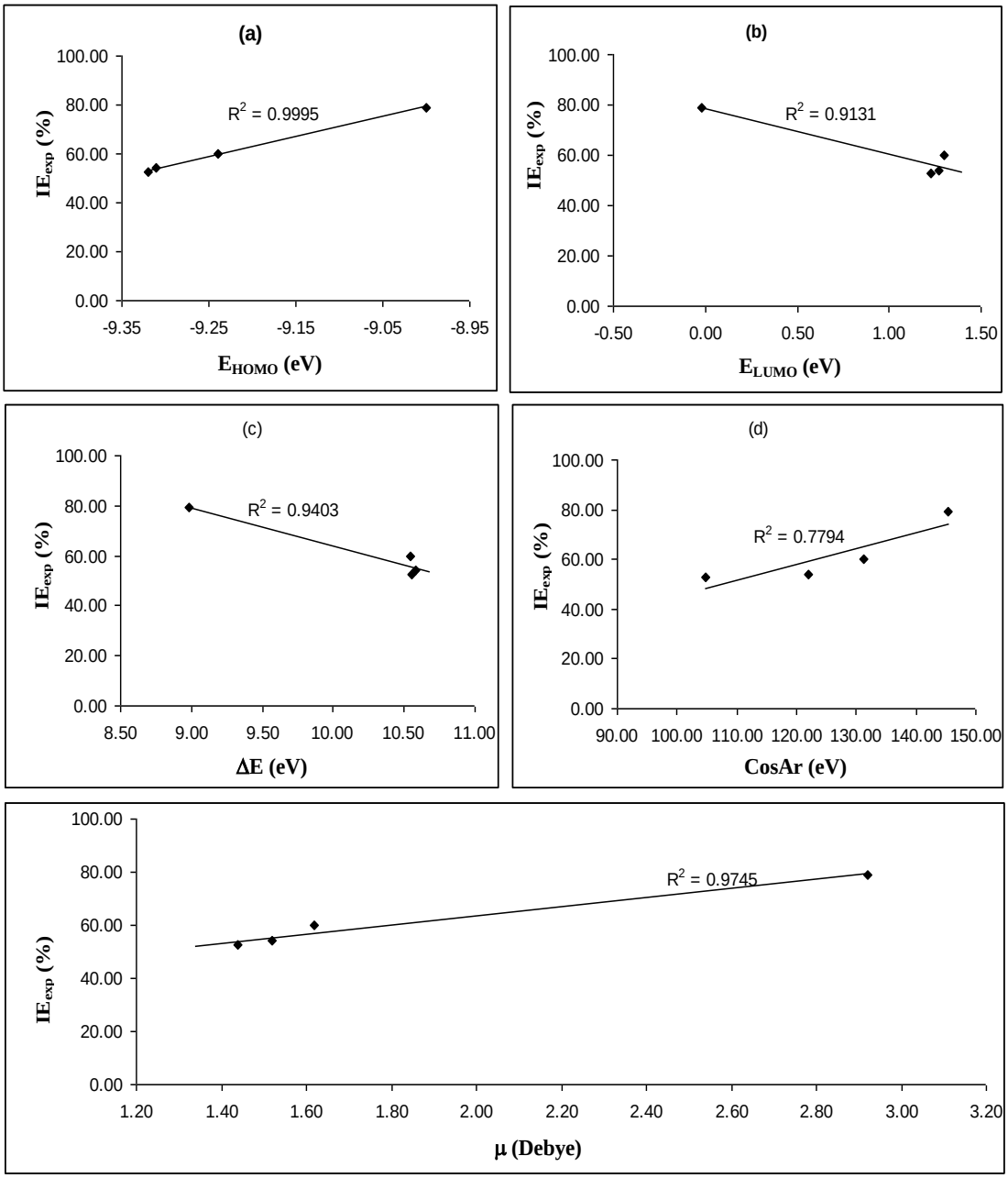

Figure 6. Variation of experimental inhibition efficiency (IE_{exp}) with (a) the HOMO energy, E_{HOMO} (b) the LUMO energy, E_{LUMO} (c) the energy gap, ΔE (d) the cosmo area, cosAr and with (e) the dipole moment, μ obtained for gas phase calculations using AM1

Based on increasing value of E_{HOMO}, the order for the variation of inhibition efficiencies of the studied inhibitors (for both gas and aqueous phases) is consistent with the order obtained from experimental data (i.e CYS > LEU > ALA > GLY). However, results obtained from PM6 Hamiltonian for gas phase calculations, strongly deviate from this trend and can be explained as follow. All the semi empirical methods contain some sets of parameters. Atomic and diatomic parameters exist in PM6, while MNDO, AM1, PM3, and MNDO-*d* use only single-atom parameters. Not all parameters are optimized for all methods; for example, in MNDO and AM1 the two electron one center integrals are normally taken from atomic spectra. Therefore, atomic and diatomic parameters (which are not present in PM6 model) may be significant in predicting the reactivity of the studied amino acids. Also, the E_{LUMO} measures the tendency of a molecule to accept electron. Therefore, decreasing value of E_{LUMO} suggests better inhibition efficiency [33]. From the results obtained for E_{LUMO} in gas and aqueous phases, the expected trend for the decrease in inhibition potentials of the studied amino acids is CYS > LEU > ALA > GLY. This trend supports experimental results.

Another quantum chemical parameter that was found to have excellent correlation with IE_{exp} is the ΔE (energy gap), defined as the difference between E_{LUMO} and E_{HOMO} [34]. According to Eddy [35], the ΔE is related to the hardness and softness of a molecule because a soft molecule has a low ΔE while a hard molecule has a large ΔE. Consequently, a soft molecule is expected to be more reactive than a hard molecule due to the smaller ΔE between the last occupied orbital and the first virtual orbital. This also implies that for a soft molecule, the ease in which intermolecular electron transfer can proceed is appreciable. Therefore, inhibition efficiency of the studied amino acids is expected to increase with decreasing value of ΔE. This assertion supports the results obtained from experiments. Fig. 6 shows the variation of IE_{exp} with some gas phase AM1 quantum chemical parameters. From the figures, it can be seen that there is a strong correlation between IE_{exp} and the frontier molecular orbital energies (i.e E_{HOMO}, E_{LUMO} and ΔE). Similar plots developed for aqueous phase calculations and for other Hamiltonians also indicated strong correlation. However, the plots are not presented but values of R^2 obtained from the plots are recorded in Table 3.

The electronic energy of the molecule (EE), core core repulsion energy (CCR), heat of formation (H_f), cosmo area (cosAr) and cosmo volume (cosVol) were also calculated. These parameters have been found to be useful in predicting the direction of a corrosion inhibition reaction for some systems [36]. However, in this study, only the cosAr (obtained for aqueous phase calculations) correlated strongly with the IE_{exp}, therefore data for EE, CCR, H_f and cosVol are not presented in Table 3.

The μ (dipole moment) is an index suitable for the prediction of the direction of a corrosion inhibition process. μ is the measure of polarity in a bond and is related to the distribution of electron in a molecule [37]. Although literature is inconsistent on the use of 'μ' as a predictor for the direction of a corrosion inhibition reaction, it is generally agreed that the adsorption of polar compounds possessing high μ on the metal surface should lead to better inhibition efficiency. Comparison of the results obtained from quantum chemical calculations (for both gas and aqueous phases) with IE_{exp} revealed that the inhibition efficiencies of the inhibitors increase with increasing value of μ.

Aqueous phase calculations also yielded values for the dielectric energy of the molecules (E_{diel}). These values also correlated excellently with IE_{exp}.

3.5.2. DFT study

DFT is one of the most power tools in quantum chemistry. It is based on the principle that the energy of a molecule can be determined from the electron density instead of using the wave function [38]. The DFT based on the Hohnenberg-Kohn theorems has been found to be a significant tool for the modelling and development of conceptual issues on chemical reactivity [39]. In corrosion study, DFT has also been used for the prediction of the sites for electrophilic and nucleophilic attacks [40]

According to Stoyanov *et al*. [41], in DFT, the ground state energy of an atom or a molecule is expressed in terms of its electron density ρ(r). Two chemical reactivity indices, namely chemical potential (ϒ) and global hardness (η) are defined as the first and second derivative of TE(ρ) with respect to the number of electrons, Thus,

$$\Upsilon=[\delta TE/\delta N]_v \quad (11)$$

$$\eta=(\delta^2 TE/\delta N^2)_{V(r)} = \tfrac{1}{2}(\delta\Upsilon/\delta N)_{V(r)} \quad (12)$$

where TE is the total energy, η is the global hardness and N is the number of electrons in the molecule. The global softness (S) is the inverse of the η and is defined as S = ½ η. From the application of the finite difference approximation, the η and S were evaluated using the following equations [42]

$$\eta=[(E_{(N-1)} - E_{(N)}) - (E_{(N)} - E_{(N+!)})] \quad (13)$$

$$S=1/[(E_{(N-1)} - E_{(N)}) - (E_{(N)} - E_{(N+!)})] \quad (14)$$

where $E_{(N-1)}$, $E_{(N)}$ and $E_{(N+1)}$ are the ground state energies of the molecule with N-1, N and N+1 electrons respectively. Also, the ionization energy (IE) and the electron affinity (EA) of the molecules were calculated using the ground state energies of the respective systems as follows [43],

$$IE=E_{(N-1)} - E_{(N)} \quad (15)$$

$$EA=E_{(N)} - E_{(N+!)} \quad (16)$$

Comparing equations 13 and 14 with equations 15 and 16 respectively, the η and S can be expressed as follow,

$$\eta=IE - EA \quad (17)$$

$$S=1/[(IE - EA)] \quad (18)$$

Calculated values of IE, EA, η and S for aqueous and gas phases are presented in Table 4. From the results obtained, it can be seen that the IE and the EA for the inhibitors decrease in the order

that is consistent with the experimental inhibition efficiency. It should be noted that the EA values for all the inhibitors (except that of CYS) were negative indicating the tendency of the molecule to be electrophilic.

The η and S of a molecule are DFT parameters that have been found to exhibit excellent relationship with the ΔE. Therefore, as expected, the best inhibitor (CYS) is the inhibitor with the lowest value of global hardness but least value of global softness for both gas and aqueous phases as shown in Table 4.

Electronegativity (χ) denotes the tendency of an atom in a molecule to attract the shared pair of electron towards themselves.

Table 4. Derived quantum chemical descriptors for the studied amino acids in gas and aqueous phases

Inhibitor	Gas phase								Aqueous phase						
	Models	E_N (eV)	IE (eV)	EA (eV)	χ (eV)	S (/eV)	η (eV)	δ	E_N (eV)	IE (eV)	EA (eV)	χ (eV)	S(/eV)	η (eV)	δ
CYS	PM6	-1399.28	8.40	0.97	4.68	0.13	7.43	0.16	-1399.93	5.80	3.86	4.83	0.52	1.94	0.56
	PM3	-1398.64	8.34	0.71	4.52	0.13	7.63	0.16	-1399.09	5.35	3.38	4.37	0.51	1.97	0.67
	AMI	-1522.57	8.67	0.45	4.56	0.12	8.22	0.15	-1523.04	6.07	3.02	4.54	0.33	3.05	0.40
	RMI	-1506.03	9.01	0.28	4.64	0.11	8.73	0.13	-1506.48	6.40	2.93	4.67	0.29	3.47	0.34
	MNDO	-1562.75	9.06	-0.45	4.30	0.11	9.51	0.14	-1563.15	6.17	2.16	4.16	0.25	4.01	0.35
GLY	PM6	-1075.40	8.41	-0.54	3.93	0.11	8.95	0.17	-1075.84	5.43	3.03	4.23	0.42	2.40	0.58
	PM3	-1063.68	8.16	-1.21	3.48	0.11	9.37	0.19	-1063.96	4.99	2.22	3.61	0.36	2.77	0.61
	AMI	-1173.05	8.65	-1.19	3.73	0.10	9.84	0.17	-1173.37	5.59	1.42	3.51	0.24	4.17	0.42
	RMI	-1164.57	8.46	-1.22	3.62	0.10	9.68	0.17	-1164.90	5.43	2.20	3.81	0.31	3.23	0.49
	MNDO	-1178.42	9.09	-0.65	4.22	0.10	9.74	0.14	-1178.72	5.99	2.27	4.13	0.27	3.72	0.39
LEU	PM6	-1674.71	8.21	-0.02	4.10	0.12	8.23	0.18	-1175.14	5.61	2.98	4.29	0.38	2.63	0.51
	PM3	-1661.64	8.02	-0.69	3.67	0.11	8.71	0.19	-1661.91	5.23	2.16	3.69	0.33	3.07	0.54
	AMI	-1795.93	8.42	-1.09	3.66	0.11	9.51	0.18	-1796.24	5.76	2.07	3.91	0.27	3.69	0.42
	RMI	-1780.22	8.27	-0.73	3.77	0.11	9.00	0.18	-1780.53	5.63	2.12	3.88	0.28	3.51	0.45
	MNDO	-1803.27	8.86	-0.59	4.13	0.11	9.45	0.15	-1803.56	6.15	2.20	4.17	0.25	3.95	0.36
ALA	PM6	-1225.30	8.43	-0.10	4.16	0.12	8.53	0.17	-1225.76	5.58	3.00	4.29	0.39	2.58	0.53
	PM3	-1213.20	8.13	-0.72	3.71	0.11	8.85	0.19	-1213.47	5.17	2.17	3.67	0.33	3.00	0.55
	AMI	-1328.73	8.56	-0.81	3.88	0.11	9.37	0.17	-1329.04	5.71	2.08	3.89	0.28	3.63	0.43
	RMI	-1318.61	8.41	-0.75	3.83	0.11	9.16	0.17	-1318.92	5.58	2.14	3.86	0.29	3.44	0.46
	MNDO	-1334.69	8.96	-0.16	4.40	0.11	9.12	0.14	-1334.97	6.05	2.22	4.13	0.26	3.83	0.37

Calculated values of χ for the inhibitors in gas and aqueous phases are also presented in Table 4. The results indicate that the best inhibitor had the highest value of χ while the least value of χ was exhibited by the inhibitor that has the least IE_{exp}.

The fraction of electron transferred, δ was calculated using equation 19 [44],

$$\delta = (\chi_{Fe} - \chi_{inh})/2(\eta_{Fe} + \eta_{inh}) \quad 19$$

where χ_{Fe} and χ_{inh} are the electronegativity of Fe and the inhibitor respectively while η_{Fe} and η_{inh} are the global hardness of Fe and the inhibitor respectively. In this study, the theoretical values of χ_{Fe} = 7ev and η_{Fe} = 0 were used for the computation of δ values for the various Hamiltonians. The results obtained from gas and aqueous phases calculations for δ values of the studied amino acids indicated that the fraction of the electron transferred were approximately similar indicating that the differences between the inhibition efficiencies of the studied amino acids can not be attributed to δ values alone.

3.5.3. Local selectivity

The merit behind the Fukui function is that it provides an avenue for analysing the local selectivity of a corrosion inhibitor [45]. The Fukui function can be defined as follows,

$$f(r) = [(\delta\Upsilon/\delta\nu(r))]_N \quad 20$$

where $\nu(r)$ is the external potential, whose functional derivative must be taken at constant number of electrons. Assuming $[\delta TE/\delta N]_\nu$ and $[\delta TE/\delta\nu(r)]_N$ are exact differentials, then the Maxwell relations between the derivatives can be written as follows,

$$f(r) = [(\delta\rho(r)/\delta N)]_\nu \quad 21$$

According to Fuentealba *et al*. [46], equation 21 is the most standard presentation of the Fukui function. However, owing to the discontinuity of the chemical potential at integer N, the derivative will be different if taken from the right or the left side. Therefore three different forms of Fukui functions (f^+,f^0 and f^-) are possible. These correspond to the situation when N increase from N to N+1(f^+) and when N decreases from N to N-1 (f^-). f^o is associated with the LUMO and measures the reactivity towards a donor reagent while f^- is associated with the HOMO and measures the reactivity toward an acceptor reagent. However, the average of both measures reactivity towards a radical. In this work, the finite difference approximation was used to calculate the electrophilic and nucleophilic Fukui function as follows,

$$f^+ = (\delta\rho(r)/\delta N)^+_\upsilon = q_{(N+1)} - q_{(N)} \quad 22$$

$$f^- = (\delta\rho(r)/\delta N)^-_\upsilon = q_{(N)} - q_{(N-1)} \quad 23$$

where ρ, $q_{(N+1)}$, $q_{(N)}$ and $q_{(N-1)}$ are the density of electron and the Mulliken/Lowdin charge of the atom with N+1, N and N-1 electrons. Values of f^+ and f^- for CYS, GLY, LEU and ALA calculated for DFT-B3LYP (6-31G) and MP2 (STO-5G) models are presented in Table 5. Since there is similarity between the Fukui function and the frontier molecular orbitals, it is expected that the site for

nucleophilic attack is the site where the value of f^+ is maximum while the site for electrophillic attack is controlled by the values of f^-. From the results obtained, the site for electrophilic attack in the studied amino acids is in the amine bond (N2-C3) of the respective amino acids. On the other hand, the sites for nucleophilic attacks are in C3 atom of the respective amino acids. The observed similarity in the sites for electrophilic and nucleophilic attacks suggests similarity in mechanism of inhibition.

Table 5. Huckel charges and Fukui functions for electrophilic and nucleophilic attacks on carbon and electronegative atoms in the studied amino acids calculated from Mulliken (Lowdin) charges using DFT-B3YLP (6-31G) and MP2 (STO-5G)

Inhibitor	DFT-B3YLP (6-31G)			MP2 (STO-5G)		Huckel charge
	Atom No	f^+ (|e|)	f^- (|e|)	S^+ (eV|e|)	S^- (eV|e|)	
CYS	1 C	-0.1405(-0.1846)	-0.0323(0.0062)	-0.3016(-0.3548	0.0129(0.0245)	0.5881
	2 N	-0.0120(-0.0187)	-0.2039(-0.2966)	-0.0061(-0.0068	-0.0072(-0.0108)	-0.2506
	3 C	0.0399(0.0126)	0.0781(0.0190)	0.0083(0.0103	-0.0008(-0.0013)	0.0432
	4 C	0.0458(-0.0630)	0.0663(-0.0049)	0.0110(0.0066	0.0005(-0.0175)	-0.0600
	5 S	-0.1908(-0.1764)	-0.2980(-0.3130)	-0.0462(-0.0448	-0.5635(-0.6231)	-0.0093
	6 O	-0.1563(-0.1639)	-0.0515(-0.0477)	-0.2267(-0.2316	-0.0413(-0.0453)	-0.6751
	7 O	-0.0612(-0.0793)	-0.0046(-0.0124)	-0.0754(-0.0797	-0.0132(-0.0142)	-0.1228
GLY	1 C	-0.4288(0.0379)	-0.0418(0.0010)	-0.3083(-0.3617)	0.0004(0.0185)	0.5846
	2 N	1.5359(1.0295)	-0.3776(-0.5288)	-0.0074(-0.0087)	-0.3306(-0.4563)	-0.2412
	3 C	0.1369(0.2255)	0.1292(0.0212)	0.0093(0.0082)	0.0256(0.0130)	-0.0232
	4 O	1.0194(0.8084)	-0.0509(-0.0415)	-0.2389(-0.2444)	-0.0549(-0.0568)	-0.6574
	5 O	1.2327(0.7798)	-0.0439(-0.0519)	-0.0779(-0.0818)	-0.0271(-0.0282)	-0.1263
LEU	1 C	-0.1729(-0.2293)	-0.0458(0.0022)	-0.3048(-0.3588)	0.0008(0.0162)	0.5842
	2 N	-0.0066(-0.0140)	-0.3301(-0.4642)	-0.0052(-0.0062)	-0.3253(-0.4481)	-0.2504
	3 C	0.0494(0.0087)	0.1163(0.0193)	0.0067(0.0090)	0.0261(0.0172)	0.0348
	4 C	0.0514(-0.0126)	0.0496(-0.0216)	0.0006(-0.0056)	-0.0006(-0.0095)	-0.0538
	5 C	0.0285(-0.0022)	0.0235(-0.0019)	0.0002(-0.0005)	0.0008(-0.0006)	0.0379
	6 C	0.0545(-0.0281)	0.0169(-0.0019)	0.0022(0.0001)	0.0044(0.0025)	-0.1408
	7 C	0.0295(-0.0144)	0.0093(-0.0080)	0.0010(-0.0012)	0.0011(-0.0016)	-0.1342
	8 O	-0.1724(-0.1878)	-0.0424(-0.0359)	-0.2319(-0.2375)	-0.0461(-0.0475)	-0.6666
	9 O	-0.0712(-0.0882)	-0.0287(-0.0359)	-0.0760(-0.0799)	-0.0228(-0.0239)	-0.1352
ALA	1 C	-0.1977(-0.2179)	-0.0481(0.0018)	-0.3063(-0.3598)	-0.0011(0.0142)	0.58103
	2 N	1.5181(1.0055)	-0.3609(-0.5014)	-0.0057(-0.0067)	-0.3277(-0.4513)	-0.2487
	3 C	0.0746(0.0516)	0.1461(0.0280)	0.0084(0.0094)	0.0280(0.0180)	0.05596
	4 C	0.6893(0.6527)	0.0337(-0.0226)	0.0039(-0.0051)	0.0037(-0.0083)	-0.1184
	5 O	1.0042(0.7850)	-0.0473(-0.0402)	-0.2339(-0.2395)	-0.0446(-0.0458)	-0.6632
	6 O	1.2276(0.7671)	-0.0345(-0.0430)	-0.0765(-0.0806)	-0.0250(-0.0256)	-0.1314

The local softness is defined as the product of the Fukui function and the global softness, S and can be expressed as follows [47].

$$s^+ = (f^+)S \quad (24)$$

$$s^- = (f^-)S \quad (25)$$

Also, the relative nucleophilicity (s^+/s^-) and relative electrophilicity (s^-/s^+) are indices that is also related to the local softness and can be applied for the prediction of the sites for nucleophilic and electrophilic attacks. Although the values of the s^+/s^- and s^-/s^+ are not recorded, it was observed that both approaches gave results similar to those obtained from the Fukui function calculations.

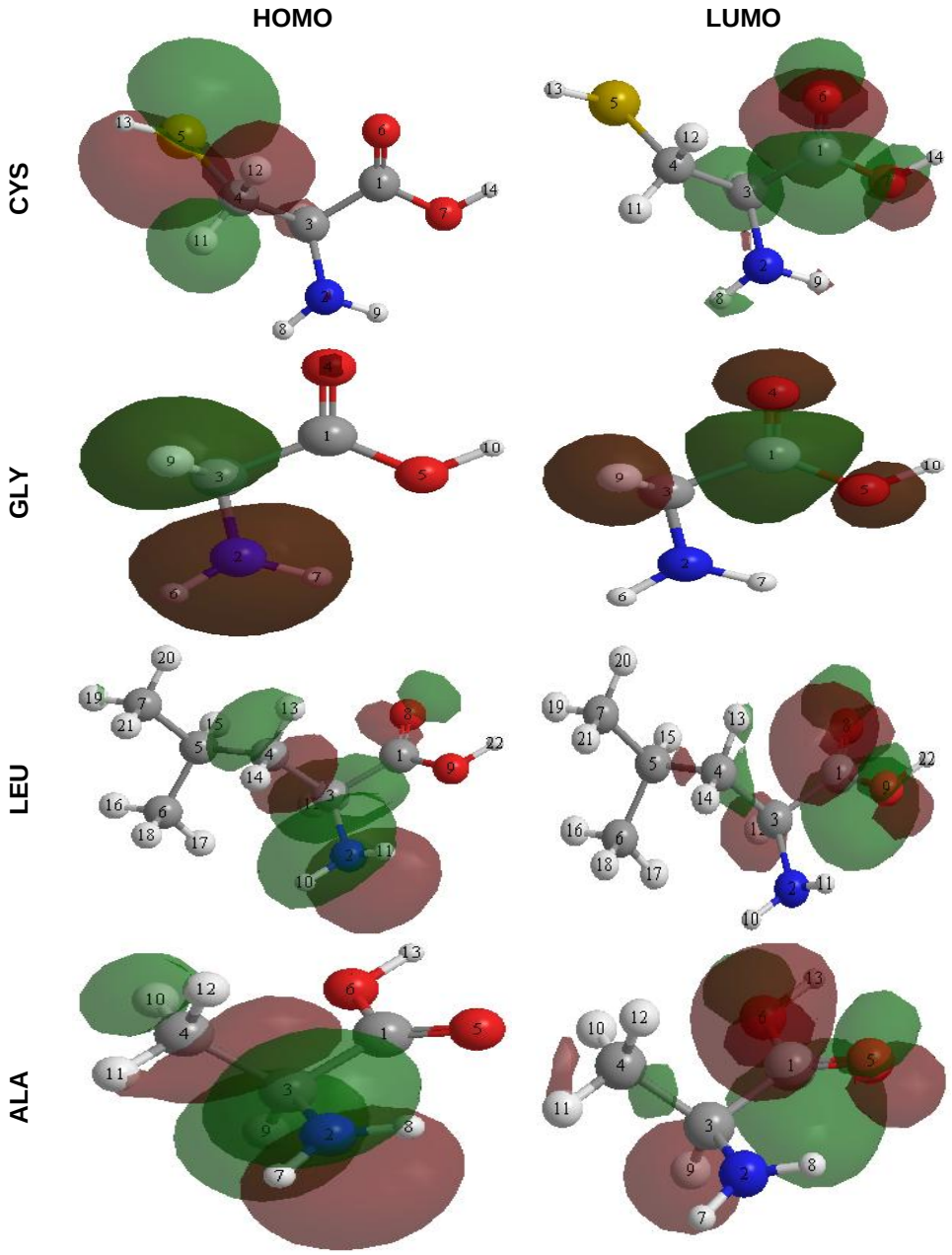

Figure 7. Extended Huckel Molecular orbital of the studied amino acids showing the HOMO and the LUMO

In Fig. 7 the molecular orbitals of the studied amino acids for the HOMO and LUMO are presented. In the orbital (green represent positive while red represent negative), it can be seen that the sites for electrophilic and nucleophilic attack obtained from Fukui calculations is consistent with what is represented in the Figure.

The Huckel charges on atoms in the molecules have been reported by Rodriguez-Valdez et al. [48] to be significant parameters that can be used to further analyzed the mechanism of corrosion inhibition. Table 5 also present Huckel charges on carbon and electronegative elements in the studied amino acids. The results reveal that the most negative charge in the studied amino acids is resident in the oxygen atoms. However, nitrogen is more electronegative than oxygen; therefore the preferred site for electrophilic attack is in the nitrogen atom of the respective inhibitor. This finding is consistent with those obtained from Fukui functions. It was also found that there is a strong correlation (R^2 = 0.9865) between experimental inhibition efficiencies and the total negative charge (TNC) on the electronegative atoms of the studied amino acids. The TNC was found to decrease according to the following trend, CYS (-1.0578) >LEU (-1.052) > ALA (-1,0434) > GLY(-1.0249) and is consistent with the trend obtained from experimental results.

3.6. Quantitative structure activity relation (QSAR) study

From the present study, it has been established that the mechanism of inhibition involves the donation of electron to Fe in mild steel by the electron. However, it has also been found that the inhibitor can not only donate electron to the metal but can also accept electron from the lone pair of Fe, leading to the formation of a feed back bond [49]. The formation of a feed back bond can be analyzed by considering a quantitative relationship between the E_{HOMO}, E_{LUMO} and the experimental inhibition efficiency. The considerations led to the establishment of equations 27 to 31 for PM6, PM3, AM1, RM1 and MNDO Hamiltonians respectively (for gas phase data).

$$IE_{exp} = 2.73E_{HOMO} - 37.43E_{LUMO} + 99.53 \quad (27)$$

$$IE_{exp} = 23.55E_{HOMO} - 21.45E_{LUMO} + 282.33 \quad (28)$$

$$IE_{exp} = 86.77E_{HOMO} - 1.25E_{LUMO} + 860.04 \quad (29)$$

$$IE_{exp} = 78.36E_{HOMO} - 29.26E_{LUMO} + 814.18 \quad (30)$$

$$IE_{exp} = 125.80E_{HOMO} - 121.83E_{LUMO} + 1402.96 \quad (31)$$

From the above equations, it can be seen that the coefficients of the E_{HOMO} are positive while that of E_{LUMO} are negative indicating that the formation of a feed back bond is favoured by increasing value of E_{HOMO} but with decreasing value of E_{LUMO}. Correlations between the above equation and the experimental inhibition efficiencies were excellent (R^2 ranges from 0.8923 to 0.9357). However, when

all the calculated quantum chemical parameters were used for developing suitable models for the different Hamiltonians (through multiple regression), it was not possible to obtain simple equations such as those given in equations 27 to 31. This indicates that the corrosion inhibition process is a composite function of some quantum chemical descriptors.

According to Lukovits *et al*. [50], the linear model approximate corrosion inhibition potentials as follows

$$IE_{Theor} = Ax_iC_i + B \qquad 32$$

where A and B are the regression coefficients determined through regression analysis, x_i is a quantum chemical index characteristic of the molecule i, C_i is the experimental concentration of the inhibitor. However, the linear model expressed by equation 32 did not give a good relationship between the experimental and theoretical inhibition efficiencies Therefore, a non linear model (equation 33), which was first proposed by Lukovits *et al*, [51] for the study of interaction of corrosion inhibitors with metal surface in acidic solutions was used. This non linear model is based on the Langmuir adsorption isotherm and can be expressed as follows,

$$IE_{Theor}(\%) = \frac{(Ax_j + B)C_i}{1 + (Ax_j + B)C_i} \times 100 \qquad 33$$

where IE_{Theor} is the theoretical inhibition efficiency, A is a regression coefficient, B is a regression constant, C_i is the experimental concentration of the inhibitor and x_i is a quantum chemical index of the molecule, i. Application of equation 33 to the present system yielded equations 34 to 38 for gas phase PM6, PM3, AM1, RM1 and MNDO Hamiltonians respectively. Similarly, equations 39 to 43 were obtained for the respective aqueous phase Hamiltonians

$$IE_{Theor} = \frac{(1.4999E_{HOMO} + 0.984E_{LUMO} + 1.0276\Delta E + \mu + 20.8235)*C \times 100}{(1+(1.4999E_{HOMO} + 0.984E_{LUMO} + 1.0276\Delta E + \mu + 20.8235)*C} \qquad 34$$

$$IE_{Theor} = \frac{(2.150E_{HOMO} + 0.409E_{LUMO} + 3.322\Delta E + \mu)*C \times 100}{(1+(2.150E_{HOMO} + 0.409E_{LUMO} + 3.322\Delta E + \mu)*C} \qquad 35$$

$$IE_{Theor} = \frac{(1.085E_{HOMO} + 1.114E_{LUMO} + \Delta E + 4.128\mu)*C \times 100}{(1+(1.085E_{HOMO} + 1.114E_{LUMO} + \Delta E + 4.128\mu)*C} \qquad 36$$

$$IE_{Theor} = \frac{(1.53E_{HOMO} + 0.549E_{LUMO} + 2.072\Delta E + \mu)*C \times 100}{(1+(1.53E_{HOMO} + 0.549E_{LUMO} + 2.072\Delta E + \mu)*C} \qquad 37$$

$$IE_{Theor} = \frac{(3.2296*E_{HOMO}+E_{LUMO}+3.7704\Delta E + 0.0245*\mu+5.4307 \times 10^{-18}) \times C \times 100}{(1+(3.2296*E_{HOMO}+E_{LUMO}+3.7704\Delta E + 0.0245*\mu+5.4307 \times 10^{-18})*C} \qquad 38$$

$$IE_{Theor}(\%) = \frac{(0.950E_{HOMO} + 1.4785E_{LUMO} + \Delta E + \mu + 0.97498E_{diel} + 11.6321)*C \times 100}{(1+((0.950E_{HOMO} + 1.4785E_{LUMO} + \Delta E + \mu + 0.97498E_{diel} + 11.6321)*C} \quad 39$$

$$IE_{Theor}(\%) = \frac{(0.860E_{HOMO} + 1.37E_{LUMO} + \Delta E + \mu + 1.193E_{diel} + 1.193 + 70.79)*C \times 100}{(1+(0.860E_{HOMO} + 1.37E_{LUMO} + \Delta E + \mu + 1.193E_{diel} + 1.193 + 70.79)*C} \quad 40$$

$$IE_{Theor}(\%) = \frac{(0.862E_{HOMO} + 1.08E_{LUMO} + 0.7356\Delta E + \mu + E_{diel} + 11.24)*C \times 100}{(1+(0.862E_{HOMO} + 1.08E_{LUMO} + 0.7356\Delta E + \mu + E_{diel} + 11.24)*C} \quad 41$$

$$IE_{Theor}(\%) = \frac{(0.896E_{HOMO} + 1.38E_{LUMO} + \Delta E + \mu + 1.649E_{diel} + 18.38)*C \times 100}{(1+(0.896E_{HOMO} + 1.38E_{LUMO} + \Delta E + \mu + 1.649E_{diel} + 18.38)*C} \quad 42$$

$$IE_{Theor}(\%) = \frac{(1.301E_{HOMO} + 0.946E_{LUMO} + \Delta E + \mu + 3.467E_{diel} + 22.28)*C \times 100}{(1+(1.301E_{HOMO} + 0.946E_{LUMO} + \Delta E + \mu + 3.467E_{diel} + 22.28)*C} \quad 43$$

Table 6. Theoretical inhibition efficiencies of the studied amino acids in gas and aqueous phases

	C (g/l)	Gas phase						Aqueous phase			
		Inhibition efficiency (%)						**Inhibition efficiency (%)**			
		PM6	PM6	PM3	AM1	RM1	MNDO	PM3	AM1	RM1	**MNDO**
CYS	0.1	65.86	87.70	50.96	63.71	63.71	58.24	54.85	53.11	45.29	**48.13**
	0.2	79.42	93.45	67.51	77.83	77.83	73.61	70.84	69.38	62.35	**64.98**
	0.3	85.27	95.54	75.71	84.04	84.04	80.71	78.47	77.26	71.29	**73.57**
	0.4	88.53	96.61	80.61	87.53	87.53	84.7	82.93	81.92	76.81	**78.77**
	0.5	90.53	97.27	83.86	89.77	89.77	87.46	85.87	84.99	80.54	**82.27**
	R^2	0.9518	0.9565	0.9572	0.9591	0.9584	0.9407	0.9578	0.9538	0.9530	**0.9544**
GLY	0.1	66.05	87.81	50.22	63.26	63.26	50.53	60.92	49.32	48.56	**50.53**
	0.2	79.56	93.51	66.86	77.5	77.50	67.14	75.71	66.06	65.37	**67.13**
	0.3	85.37	95.58	75.16	83.78	83.78	75.39	82.38	74.49	73.9	**75.39**
	0.4	88.61	96.65	80.14	87.32	87.32	80.34	86.18	79.56	79.06	**80.33**
	0.5	90.88	97.3	83.45	89.59	89.59	83.63	88.63	82.95	82.52	**83.62**
	R^2	0.9053	0.9121	0.9299	0.9311	0.9281	0.8721	0.9285	0.9083	0.9083	**0.9280**
LEU	0.1	66.58	87.69	48.74	61.76	61.76	51.83	61.37	52.75	49.55	**50.99**
	0.2	79.94	93.44	65.54	76.36	76.36	68.28	76.06	69.07	66.27	**67.54**
	0.3	85.67	95.53	74.05	82.89	82.89	76.35	82.66	77.01	74.66	**75.74**
	0.4	88.85	96.61	79.18	86.59	86.59	81.15	86.4	81.71	79.71	**80.63**
	0.5	90.68	97.27	82.62	88.98	88.98	84.33	88.82	84.81	83.08	**83.88**
	R^2	0.8985	0.9108	0.9241	0.9282	0.9270	0.8732	0.9305	0.9102	0.9102	**0.9256**
ALA	0.1	65.66	87.78	50.12	62.67	62.67	50.69	61.21	50.57	49.15	**50.79**
	0.2	79.27	93.49	66.77	77.05	77.05	67.27	75.94	67.17	65.91	**67.36**
	0.3	85.15	95.57	75.09	83.44	83.44	75.51	82.56	75.42	74.36	**75.56**
	0.4	88.44	96.64	80.07	87.04	87.04	80.44	86.32	80.36	79.45	**80.5**
	0.5	90.61	97.29	83.4	89.35	89.35	83.71	88.75	83.65	82.86	**83.77**
	R^2	0.8616	0.8613	0.8645	0.8648	0.8646	0.8519	0.8646	0.8661	0.9606	**0.8642**

** Values of R^2 between experimental and theoretical inhibition efficiencies for each inhibitor are also included in the Table

The theoretical values of inhibition efficiencies computed from equations 34 to 43 are recorded in Table 6. In Table 6, we also present R^2 values, which were obtained from the plots of IE_{exp} versus IE_{Theor}. From the results obtained, it can be seen that there is a strong correlation between IE_{exp} and IE_{Theor} as shown in R^2 values recorded in Table 6. Fig. 8 also shows a representative plot for the variation of experimental inhibition efficiency with theoretical inhibition efficiency.

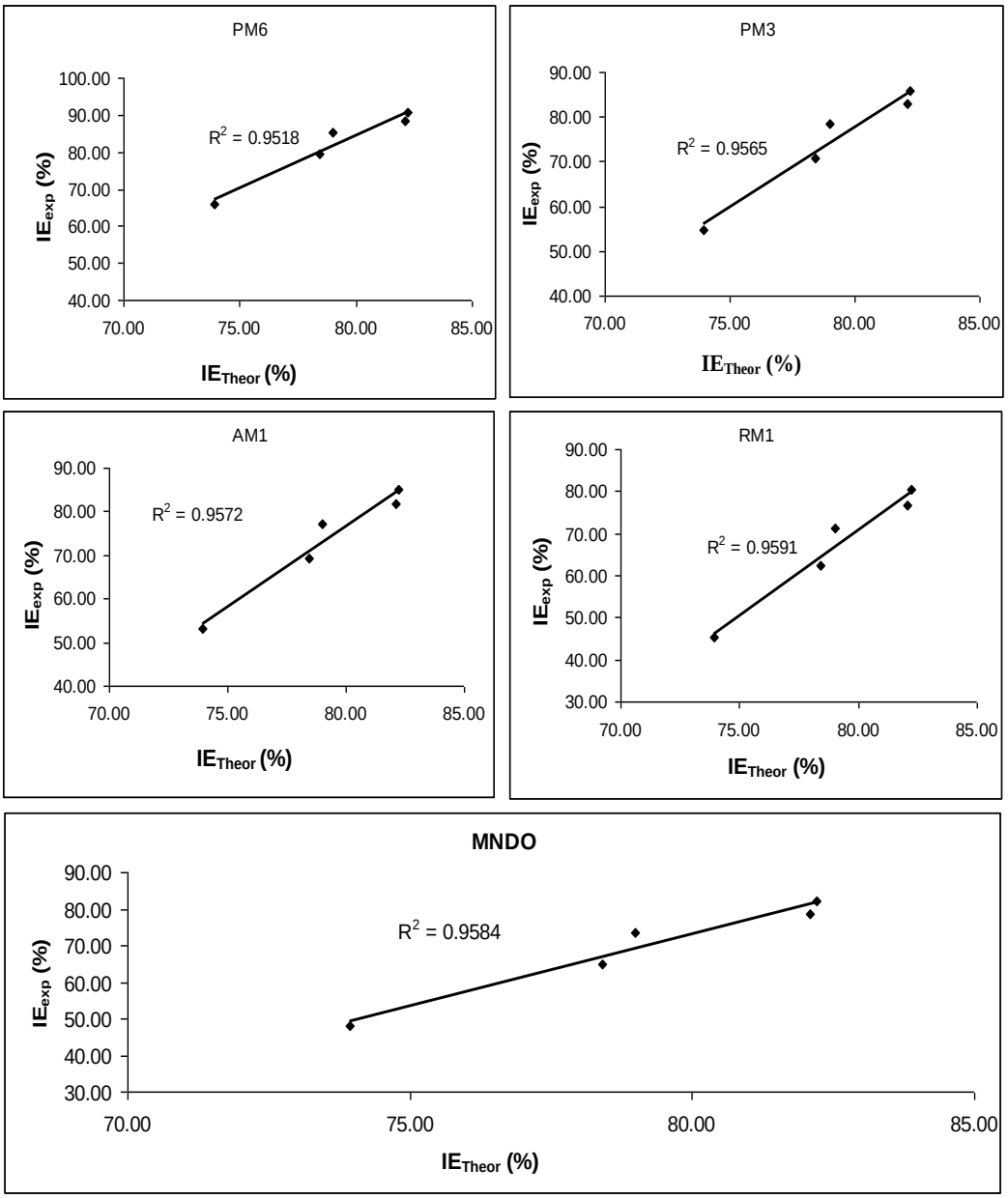

Figure 8. Variation of experimental and theoretical inhibition efficiencies of CYS in gas phase for the various Hamiltonians

3.7. Mechanism of inhibition

From the study, it has been established that the corrosion of mild in HCl solution is inhibited by various concentrations of CYS, GLY, LEU and ALA. The inhibition mechanism (for a reaction such

as the one under study), involves the blockage of mild steel surface by the inhibitor molecules via adsorption. In this study, a physical adsorption mechanism has been proposed. However, it is worth stating that after physical adsorption, the mechanism of chemical adsorption is certain. Generally, the adsorption of the inhibitor on mild steel surface can be influenced by the nature and surface charge of the metal and by the chemical structure of the inhibitor. It is evident that the four inhibitors are structurally related, Also, from Fukui indices, Huckel charges on the electronegative elements and considerations of the HOMO and the LUMO, it has been established that the sites for adsorption of the studied amino acids is in the carbonyl oxygen. In acidic medium, it is possible that the amino group of the inhibitors can be protonated to NH_3^+. This fact is supported by the fact that the maximum value of f^+ is in the amino functional group. The protonation is succeeded by formation of adsorption layer between Fe in mild steel and carbonyl functional groups in the inhibitor.

4. CONCLUSIONS

From the results and findings of the study, the following conclusions are made:

1. CYS, GLY, LEU and ALA inhibited the corrosion of mild steel through the mechanism of physical adsorption. The adsorption of the inhibitor on mild steel surface is exothermic (values of ΔH_{ads} were negative) spontaneous (values of ΔG_{ads} were negative) and supports the Langmuir adsorption model.
2. There is a strong correlation between experimental inhibition efficiencies and some quantum chemical parameters (namely, E_{LUMO}, E_{HOMO}, ΔE, $E_{dielect}$ and with μ) for both gas and aqueous phases. Correlations between experimental and theoretical inhibition efficiencies (obtained from QSAR calculations) were also excellent.
3. From FTIR data, Fukui function calculations, consideration of Huckel charges on the atoms, it is indicative that the site for electrophilic attack on the studied amino acids is at the amino nitrogen atom.
4. Therefore, QSAR can be used to model the inhibition potentials of amino acids, including CYS, LEU, ALA and GLY which are good inhibitors for the corrosion of mild steel in HCl.

ACKNOWLEDGEMENTS
The authors are grateful to all the technical staff in the Department of Chemistry, Ahmadu Bello University, for supporting the work.

References

1. G. Achary, H.P. Sachin, Y.A. Naik. T.V. Venkatesha, *Mater. Chem. Phys.* 107 (2008) 44.
2. D. Gopi, K.M. Govindaraju, V. Collins, A. Prakash, V. Manivannan, L. Kavitha , *J. Appl. Electrochem.* 39(2) (2009) 269.

3. P.C. Okafor, V. Osabor,E.E. Ebenso, *Pigment and Resin Technol.*, 36(5) (2007) 299.
4. N.O. Eddy, E.E. Ebenso, *Int. J. Electrochem. Sci.* 5 (2010) 731.
5. P.C. Okafor, E.E. Ebenso, U.J. Ekpe, *Int. J. Electrochem. Sci.* 5 (2010) 978.
6. E. Khamis, N. AlAndis, *Mat.-Wiss. u.Werkstofftech* 33(9) (2002) 550.
7. N.O. Eddy, *Port. Electrochim Acta* 27(5) (2009) 579.
8. E.E. Oguzie, A.I. Onuchukwu, P.C. Okafor, E.E. Ebenso, *Pigment and Resin Technol.* 35(2) (2006) 63.
9. E.E. Oguzie, G.N. Onuoha, E.N. Ejike, *Pigment and Resin Technol.* 36(1) (2007) 44.
10. M. Zerfaoui, H. Ouddac, B. Hammouti, S. Kertit, M. Benkaddourb, *Progress in Organic Coatings* 51 (2004) 134.
11. G. Moretti, F. Guidi, G. Grion, *Corros. Sci.* 46 (2004) 387.
12. M.A. Kiani, M.F. Mousavi, S. Ghasemi, M. Shamsipur, S.H. Kazemi, *Corros. Sci.* 50 (2008) 1035.
13. A.B. Silva, S.M.L. Agostinho, O.E. Barcia, G.G.O. Cordeiro, E. D'Elia, *Corros. Sci.* 48 (2006) 3668.
14. G. Gao, C. Liang, *Electrochimica Acta* 52 (2007) 4554.
15. A.Yurt, G. Bereket, C. Ogretir, J. Mol. Struct: THEOCHEM 725 (2005) 215.
16. H. Ashassi-Sorkhabi, Z. Ghasemi, D. Seifzadeh, *Appl. Surf. Sci* 249(2005) 408.
17. Z. Ghasemi, A. Tizpar, *Appl. Surf. Sci.* 252 (2006) 3667.
18. M. Abdallah, *Corros. Sci*, 46 (2004) 1981.
19. S.A. Umoren, O. Ogbobe, I.E. Igwe, E.E. Ebenso, *Corros. Sci.* 68(2008) 4123.
20. E.E. Ebenso, H. Alemu, S.A. Umoren, I.B. Obot, *Int. J. Electrochem. Sci.* 3 (2008) 1325.
21. S.A. Umoren, E.E. Ebenso, *Pigment and Resin Technol*, 37(3) (2008) 173.
22. E.E. Oguzie, *Pigment and Resin Technol,* 34(6) (2005) 321.
23. Steward JP. MOPAC Steward computational Chemistry. 2009. Version 9.069W. HTTP://OpenMOPAC.net
24. M.W. Schmidt, K.K. Baldridge, J.A. Boatz, S.T. Elbert, M.S. Gordon, J.H. Jensen, S. Koseki, et al., Games version 12, *J. Comp. Chem.* 1993) 1347.
25. N.O. Eddy, P.A.P. Mamza , *Port. Electrochim Acta* 27(2) (2009) 20.
26. E.A. Noor, *J. Appl. Electrochem.* 39 (2009) 1465.
27. N.O. Eddy, E.E. Ebenso, *Pigment and Resin Technol.* 39(2) (2010) 77.
28. B.I.Ita, *Bull. Electrochem.* 21(7) (2005) 219.
29. N.O. Eddy, B.I.Ita, *J. Mol. Mod.* 2010; DOI:10.1007/s00894-010-0731-7.
30. M.A. Quraishi, I. Ahamad, A.K.S. Sudhish, K.S.B. Lal , V. Singh, *Mater. Chem. Phys.* 112(2008) 1035.
31. N.O. Eddy, S.A. Odoemelam, *Pigment and Resin Technol.* 38(2) (2009) 111.
32. N.O. Eddy, S.A. Odoemelam, A.O. Odiongenyi, *J. Appl. Electrochem.* 39(6) (2009) 849.
33. H. Tanak, M. Yavuz, *J. Mol. Mod.* 16 (2010) 235.
34. M. Sahin, G. Gece, F. Karci, S. Bilgic, *J. Appl. Electrochem.* 38 (2008) 809.
35. N.O. Eddy, *Mol. Simul.* 35(5) (2010) 354.
36. V.G. Maltarollo, P. Homem-de-Mello, K.M. Honorio, *J. Mol. Mod.* 16 (2010) 799.
37. H.E. El Ashry, A. El Nemr, S.A. Esawy, S. Ragab, *Electrochimica Acta* 51 (2006) 3957.
38. T. Arslan, F. Kandemirli, E.E. Ebenso, I. Love, H. Alemu, *Corros. Sci.* 51 (2009) 35.
39. D.C. Young, Computational Chemistry, A practical guide for applying techniques to real world problems. Wiley Interscience, New York, 2001, 324.
40. N.O. Eddy, U.J. Ibok, E.E. Ebenso, A. El Nemr, H. El Ashry, *J. Mol. Mod.* 15 (2009) 1085.
41. S.R. Stoyanov, S. Gusarov, S.M. Kuznick, A. Kovalenko, *J. Phys. Chem. C.* 112(2008) 6794.
42. N.O. Eddy, E.E. Ebenso, *J. Mol. Mod.* 16 (2010) 1291.
43. S.R. Stoyanov, J.M. Villegas, D.P. Rillema, *Inorg. Chem.* 42 (2003) 7852.

44. B. Gomez, N.V. Likhanova, M.A. Dominguez, R.A. Martinez-Palou, A. Vela, J.L. Gazquez, *J. Phy. Chem. B.* 110 (2006) 8928.
45. H. Wang, X. Wang, H. Wang, L. Wang, A. Liu, *J. Mol. Mod.* 13 (2007) 147.
46. P. Fuentealba, P. Perez, R. Contreras, *J. Chem. Phys.* 113(7) (2000) 2544.
47. N.O. Eddy, B.I.Ita, *Intern. J. Quant. Chem.* 2010; DOI: 10.1002/qua
48. L.M. Rodriguez-Valdez, W. Villamisar, M. Casales, J.G. Gonzalez-Rodriguez, A. Martinez Villafane, L. Martinez L, et al., *Corros. Sci.* 48 (2006) 4053.
49. N.O. Eddy, U.J. Ibok, E.E. Ebenso, *J. Appl. Electrochem.* 40 (2010) 445.
50. I.Lukovits, I. Bakó, A. Shaban, E. Kálmán, *Electrochimica Acta* 43 (1998) 131.
51. I.Lukovits, A. Shaban, E. Kalman, Russian J. Electrochem. 39 (2003) 177.